9th ANKARA INTERNATIONAL AEROSPACE CONFERENCE **AIAC-2017-022**
20-22 September 2017 - METU, Ankara TURKEY

UNSTEADY SOLUTION OF QUASI-1D NOZZLE USING LINEARIZED HARMONIC METHOD

Arash Karshenass* and Ozgur Ugras Baran†
TED University
Ankara, Turkey

Mehmet Haluk Aksel‡
Middle East Technical University
Ankara, Turkey

ABSTRACT

The aim of this study is to develop a simple model for understanding of how harmonic methods can be applied into periodic problems without concerning geometry and mesh complexity of turbomachines. So, a quasi-1D inviscid flow through a converging-diverging nozzle is studied with a harmonically-alternating back pressure as boundary condition with definite frequency and amplitude. Steady state solution is obtained by time averaged back pressure and coupled with harmonic solver, which is based on linearized Euler methods to solve perturbation effects. Harmonic and steady-state solutions are consolidated to achieve time-accurate solution. Linearized method is employed to solve with both perturbed fluxes and primitive variables. Control volume scheme with flux splitting and local time-stepping are employed in both steady and perturbation solutions for acceleration and convergence improvement.

INTRODUCTION

Dependency of aerospace and aeronautic industries on Computational Fluid Dynamics (CFD) analysis is unavoidable. In recent years it has become more attractive than ever thanks to significant growth of available computation power. However, the demand for computational power with even higher capabilities still exist, followed by complicated mathematical methods to deal with more complex physical phenomena. From CFD point of view, current status of computers is acceptable for most steady problems. However when it comes to unsteady calculations, it is often insufficient for complex problems in industrial design process. This issue is more prominent when it comes to turbomachinery and aeroelasticity studies where required calculation effort reaches to its peak due to simultaneous contribution of several physical events. As an example, [McMullen, 2003] has reported that a study in 2001 had done in U.S. Department of Energy Defense Programs with contribution of Stanford University on time-accurate unsteady analyzes over a turbine and a compressor in a massively-parallel computer with 750 CPUs. Running details are provided in Table 1 and shows that it is not applicable to industrial applications. One way to overcome this problem is to adopt improved, and usually more complicated, mathematical methods that require less processes of calculation, instead of looking for more computation power

*Research Assistant, Email: arash.karshenass@tedu.edu.tr
†Assistant Professor, Email: ozgur.baran@tedu.edu.tr
‡Professor, Email: aksel@metu.edu.tr

to use.

Table 1: Details of the time-accurate study

Unit	Blade Rows	Grid Points	Execution Time
Turbine	9	94 million	500 days
Compressor	23	N.A.	1300 days

Unsteady solutions inside passages of a turbomachine is periodic both in time and space. It is possible to define periodic boundaries for space in steady solutions to truncate a row into a single passage for periodicity but it is not applicable in unsteady solutions. Therefore, unsteady Euler equations must be solved within whole passages by employing established time-accurate algorithm in CFD. Following that, solution within domain varies periodically in time, as shown in Figure 1.

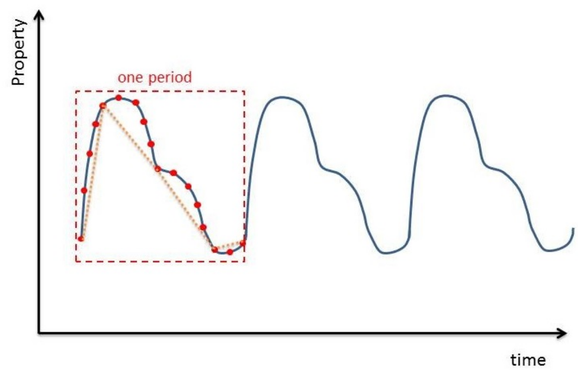

Figure 1: Periodic Solution

However, these periodic solutions cannot be achieved quickly in iterations but an initial transient solution must be run out to lead to periodic ones as shown in Figure 2. It means that required number of time-steps of transient part is significantly large compared to those for a period of solution, about 95% [Mitchell, 1995; Yao et al., 2001]. Hence, massive part of process is associated with this useless transient part and consequently is an inefficient method.

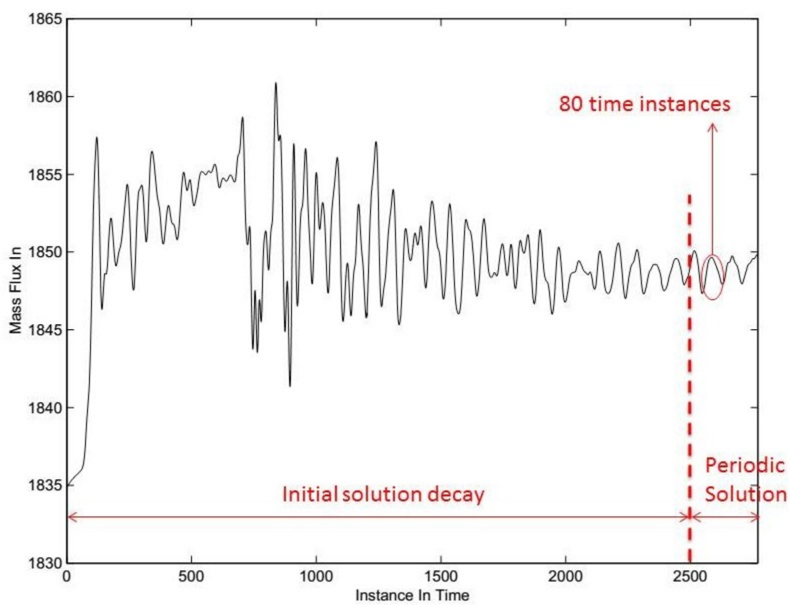

Figure 2: Decay of initial transition

On the other hand, it is possible to represent governing equations in a more suitable form by temporal periodic essence. In this periodic approach, new form of equations with temporal periodic nature can be solved in the frequency domain rather than time domain which have steady form and consequently makes it possible in turbomachinery to truncate a row into a single passage for its spatial periodicity. In periodic approach, Fourier series (as trigonometric interpolant) is used to represent the solution in time with the aim of eliminating the time-dependent parameters in governing equations and obtaining perturbed solution from time-independent perturbed equations that only rely on frequency. While number of governing equations which have to be solved simultaneously increase two or three times, the method benefits from lower computational cost since time marching calculations are avoided.

Generally, there exist three methods in periodic approach for solving compressible flow equations in frequency domain, linearized, nonlinear [Adamczyk and Goldstein, 1978] and fully nonlinear [Hall et al., 2002] methods, which are also called time-linearized, deterministic-stress and harmonic balance methods, respectively. These methods are categorized in Figure 3 with their specifications given in Table 2. All these methods are based on separation of unsteady periodic solution into a mean solution plus perturbed harmonic solution(s) about the values of mean solution [Ni and Sisto, 1976].

$$W_{(x,t)} = \overline{W}_{(x)} + \widetilde{W}_{(x,t)}$$

Where $\bar{W}$, $\tilde{W}$ and W stand for mean, perturbed harmonic and unsteady variables, respectively.

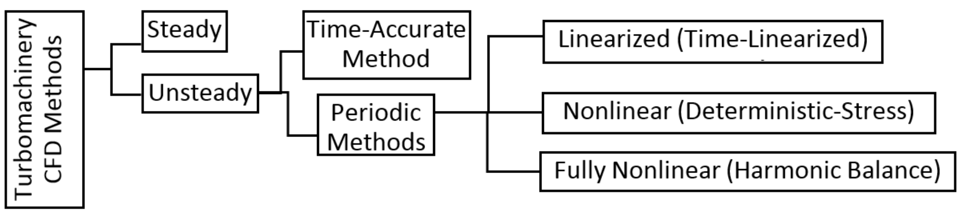

Figure 3: Turbomachinery CFD methods

Table 2: Unsteady methods specifications

Unsteady Method	Assumption of Single Pasage	Assumption of Periodicity in Time	Linear/ Nonlinear	Single/Multi Distortion	Domain to be Used
Time-Accurate	✗	✗	Nonlinear	Multi	Only time
Time-Linearized	✓	✓	Linear	Single	Time and Frequency
Deterministic Stress	✓	✓	Nonlinear	Single	Time and Frequency
Harmonic Balance	✓	✓	Nonlinear	Multi	Only Frequency

In time-linearized and deterministic-stress methods, only one disturbance with specific frequency in flow is considered. While the latter considers nonlinearities in flow such as shock waves, the prior is entirely linear and any nonlinearity cannot be captured.Consequently, magnitude of perturbed solution should be sufficiently small compared to mean solution for having linear behavior. Since time-linearized method is linear, it is possible to use superposition to sum multiple distortions with different frequencies, which are solved separately. In harmonic balance method, there can be several disturbances with different frequencies in addition to solving nonlinearities.

PROBLEM SUMMARY

The aim of this study is to develop a simple model for understanding of how harmonic methods can be applied into periodic problems without concerning geometry and mesh complexity of turbomachines. To do that, compressible flow at a subsonic quasi-1D converging-diverging nozzle is solved by linearized harmoinc method in frequency domain, Figure 4. Source of periodic pattern is harmonically-alternating back pressure with known a priori frequency and amplitude as periodic boundary condition. Following that, problem is reduced to steady and harmonic perturbation solutions, which are combined to calculate unsteady solution; hence, steady-state accelerating techniques can be applied.

Since inlet of nozzle is subsonic, two physical boundary values are required for the inlet and the third boundary condition is numeric. Stagnation pressure and density are specified at inlet while velocity is extrapolated. For the exit of nozzle, one physical boundary condition, back pressure, and two numeric boundary conditions, velocity and density, are required.

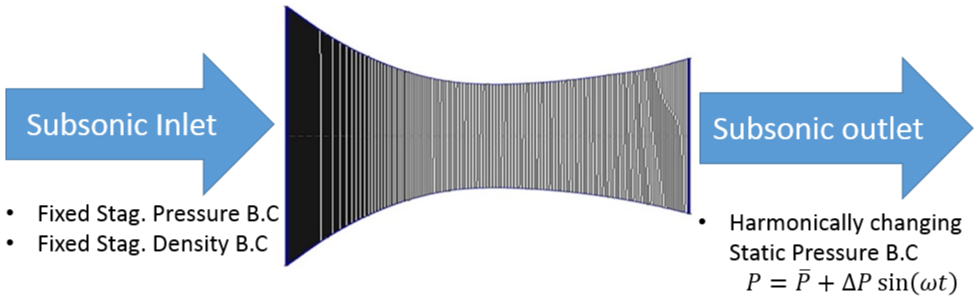

Figure 4: Geometry and mesh structure of quasi-1D nozzle

Equations defining nozzle area are $A = 1 + 1.5(1 - 2X)$ for $0 < x < 1/2$ and $A = 1 + 0.5(1 - 2x)$ for $1/2 < x < 1$. Outlet pressure of nozzle varies harmonically in time as $P = \bar{P} + \Delta P \sin(\varpi t)$ where $\varpi$is is angular speed (angular frequency) and ΔP is the amplitude of variation from the mean value $\overline{P}$. In order to have subsonic flow through nozzle, boundary values are set as $P_{0inlet} = 1.75MPa$, $\rho_{0inlet} = 17^{kg}/_{m^3}$, $\bar{P} = 1.55MPa$ (ratio of static back pressure to static inlet pressure is 0.92), $\Delta P = 7753$ (amplitude of pressure distortion is 0.5% of mean back pressure) and $\varpi = 1$. Finally, results of time-Linearized method are compared to those of time-marching method obtained from ANSYS Fluent.

METHOD

Unsteady quasi-1D Euler equation is:

$$\frac{\partial}{\partial t}\int W d\Omega + \int \vec{F}.d\vec{A} = \int S dA \quad ; \quad W = \begin{bmatrix} \rho \\ \rho u \\ \rho E \end{bmatrix} \quad ; \quad F = \begin{bmatrix} \rho u \\ \rho u^2 + P \\ (\rho E + P)\, u \end{bmatrix} \quad ; \quad S = \begin{bmatrix} 0 \\ P \\ 0 \end{bmatrix}$$

where W, F and S are conservative variables, conservative fluxes, and source terms, respectively. Source term exists due to one dimensional formulation of a two dimensional geometry and is originated from applied pressure force from walls on control volume, as Figure 5.

As the second assumption, steady state solution is considered as the mean solution, thus can be obtained from the steady state Euler equation. To solve the steady state Euler equation, spatial discretization is done by structured mesh and time discretization for pseudo-time marching is done by employing 3^{rd}order Runge-Kutta with local time stepping for acceleration. Flux Vector Splitting method (FVS) with accuracy of order 1 is utilized for flux calculations. For the variable outlet boundary condition, outlet pressure is fixed at its time averaged magnitude of π for the steady state solution.

$$\frac{\partial}{\partial \tau}\int \overline{W} d\Omega + \int \vec{\bar{F}}.d\vec{A} = \int \bar{S} dA$$

After solving for steady solution, harmonic solution should be obtained. Substituting the new definition of W into unsteady Euler equation and linearizing flux and source terms using Taylor series expansion, we get:

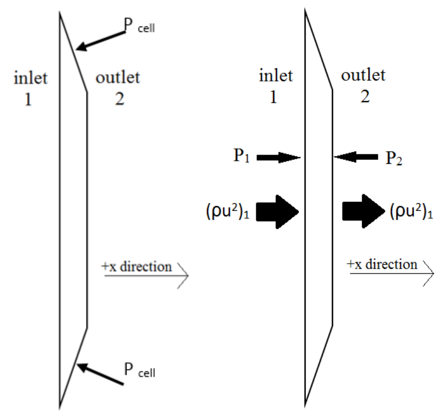

Figure 5: Momentum and forces in quasi-1D cell

$$\frac{\partial}{\partial t}\int \tilde{W} d\Omega + \int \bar{M}_F \tilde{W}.d\vec{A} = \int \bar{M}_S \tilde{W}.dA$$

where

$$\bar{M}_F = \begin{bmatrix} 0 & 1 & 0 \\ 0.5(\gamma-3)\bar{u}^2 & (3-\gamma)\bar{u} & \gamma-1 \\ \bar{u}\left((\gamma-1)\bar{u}^2-\gamma\bar{E}\right) & \frac{1}{\bar{\rho}}\left(\gamma\bar{\rho}\bar{E}-1.5(\gamma-1)\bar{\rho}\bar{u}^2\right) & \gamma\bar{u} \end{bmatrix} \quad ; \quad \bar{M}_S = (\gamma-1)\begin{bmatrix} 0 & 0 & 0 \\ 0.5\bar{u}^2 & -\bar{u} & 1 \\ 0 & 0 & 0 \end{bmatrix}$$

As the third assumption, it is assumed that the flow within domain is harmonic in time due to harmonically varying boundaries and thus solution, $\widetilde{W}$, can be represented by trigonometric interpolant such as Fourier series and consequently is a complex value. Considering only the first term in Fourier series:

$$\tilde{W}_{(x,t)} = \tilde{W}_r + \tilde{W}_i = \hat{W}_{(x)} e^{i\varpi t}$$

where $\hat{W}$ is also a complex number as $\hat{W} = \hat{W}_r + \hat{W}_i$. Thus $\tilde{W}$ can be represented as:

$$\tilde{W}_{(x,t)} = |\hat{W}_{(x)}| e^{i(\varpi t+\varphi)} \quad ; \quad |\hat{W}_{(x)}| = \sqrt{\hat{W}_r^2 + \hat{W}_i^2} \quad ; \quad \varphi = \arctan(\frac{\hat{W}_i}{\hat{W}_r})$$

This equation relates the solution in frequency domain, $\hat{W}$, to solution in time domain,$\tilde{W}$. Thus, solving $\hat{W}$ wich is independent from time will be followed by solving $\tilde{W}$. Substituting $\tilde{W}$ definition into Euler equation:

$$-i\varpi \int \hat{W} d\Omega - \int \bar{M}_F \hat{W}.d\vec{A} + \int \bar{M}_S \hat{W}.dA = 0$$

which is a time-independent equation. It is important to note that since $\hat{W}$ is a complex number, the equation will be separated into two equations, real and imaginary parts and consequently 6 simultaneous equations need to be solved for $\hat{W}_{1r}, \hat{W}_{1i}, \hat{W}_{2r}, \hat{W}_{2i}, \hat{W}_{3r}$ and $\hat{W}_{3i}$. Fluxes across cell faces are calculated based on Steger-Warming flux splitting by decomposing $\bar{M}_F$ into $\bar{M}_F^+$ and $\bar{M}_F^-$, hence fluxes are combinations of steady and perturbed variables. Since $\bar{M}_F$ is based on steady magnitudes, its eigenvalues are the same as ordinary Euler equation.

$$\hat{F}_r^{\pm} = [\bar{M}_F]^{\pm}\left\{\hat{W}_r\right\} \quad ; \quad \hat{F}_i^{\pm} = [\bar{M}_F]^{\pm}\left\{\hat{W}_i\right\}$$

RESULTS

Steady state results for aforementioned boundary values are calculated and compared to those from ANSYS Fluent for validation and are demonstrated in Figure 6.

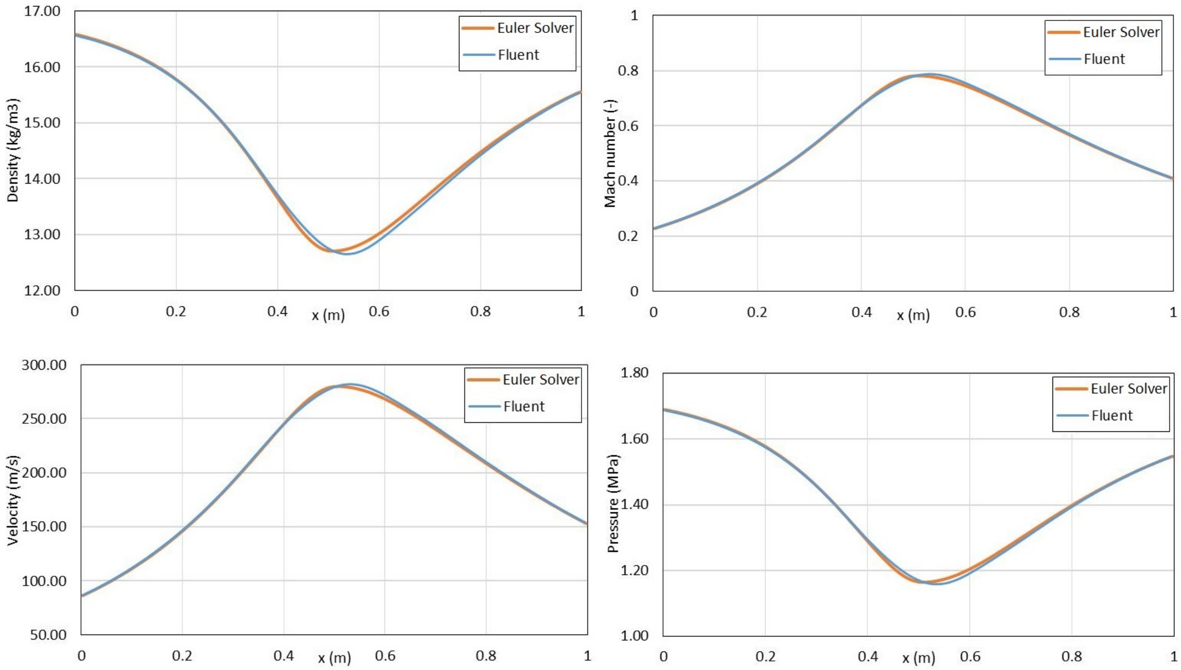

Figure 6: Steady state result comparison between developed Euler solver and steady simulations by ANSYS Fluent

Analytical solution is performed to validate both results from ANSYS Fluent and the developed code. Results from analytic method states Mach number at throat ($x = 0.5$) as 0.81 which is in good agreement with numerical results.

$$\frac{P_{out}}{P_{0out}} = 0.886 \to M_{out} = 0.412 \to \frac{A_{out}}{A*} = 1.556 \to A* = 0.964$$

A^* is the required throat area if flow would be choked. Since, throat area at the geometry is 1, thus:

$$\frac{A_{throat}}{A*} = \frac{1}{0.964} = 1.0373 \to M_{throat} = 0.81$$

For perturbed part, corresponding equations are fierst solved for $\hat{W}$ and then for $\tilde{W}$. Figure 7a shows results of perturbed $\tilde{W}$ versus x (along nozzle) for different times while Figure 7b demonstrate the same parameter versus t (along time) at different locations of the nozzle. Time period of the problem is $T = \frac{2\pi}{\omega} = \frac{2\omega}{1} = 6.28$ which means that perturbed solution repeats 6.28 seconds. Hence plots are drawn for $0 < t < 6.28$. Following that, perturbed primitive variable can be acquired, Figure 8, by applying linearization and considering only the first order perturbations.

$$W_1 = \bar{W}_1 + \widetilde{W}_1 \overset{W_1=\rho,\bar{W}_1=\bar{\rho}}{\longrightarrow} \widetilde{W}_1 = \tilde{\rho}$$

$$W_2 = \bar{W}_2 + \widetilde{W}_2 = \rho u = (\bar{\rho} + \tilde{\rho})(\bar{u} + \tilde{u}) = \bar{\rho}\bar{u} + \bar{\rho}\tilde{u} + \tilde{\rho}\bar{u} \overset{\bar{W}_2=\bar{\rho}\bar{u}}{\longrightarrow} \widetilde{W}_2 = \bar{\rho}\tilde{u} + \tilde{\rho}\bar{u} \to \tilde{u} = \frac{\widetilde{W}_2 - \tilde{\rho}\bar{u}}{\bar{\rho}}$$

similarly:

$$\tilde{E} = \frac{\widetilde{W}_3 - \tilde{\rho}\bar{E}}{\bar{\rho}} \quad ; \quad \tilde{P} = (\gamma - 1)\left(\widetilde{W}_3 - \bar{u}\widetilde{W}_2 + \frac{\bar{u}^2}{2}\widetilde{W}_1\right) \quad ; \quad \tilde{c} = \frac{\gamma}{2\bar{c}}\left(\frac{\tilde{P}}{\bar{\rho}} - \frac{\bar{P}\tilde{\rho}}{\bar{\rho}^2}\right) \quad ; \quad \tilde{M} = \frac{\tilde{u}}{\bar{c}} - \frac{\bar{u}\tilde{c}}{\bar{c}^2}$$

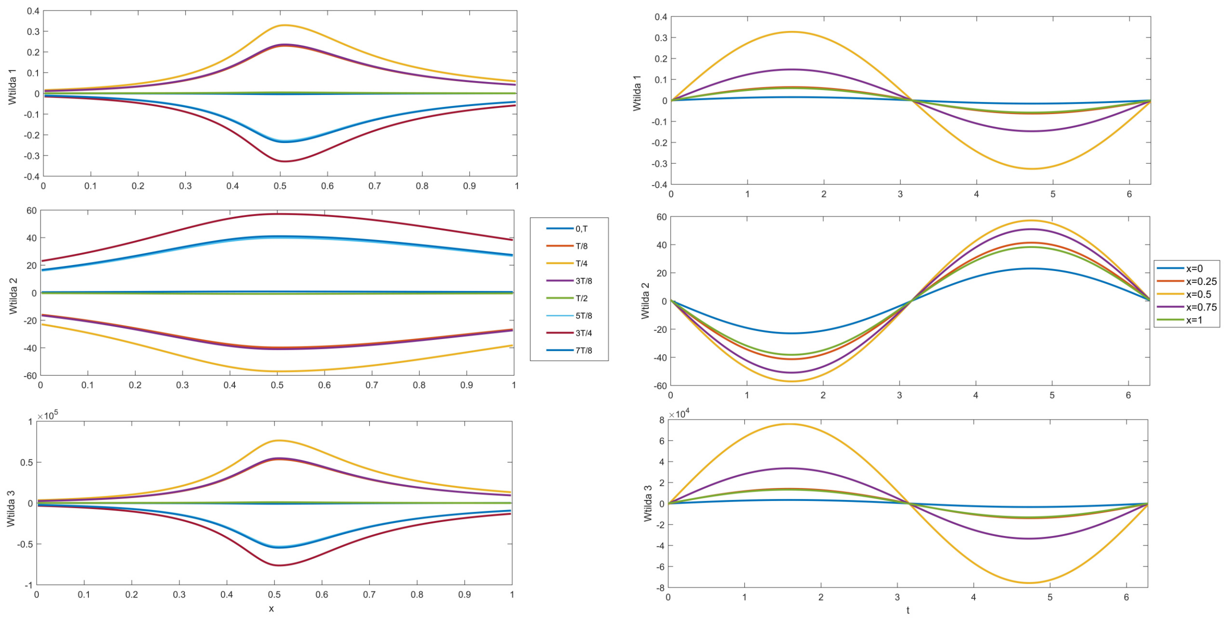

(a) along nozzle at different times (b) along time at different nozzle locations

Figure 7: Perturbed conservative variables from harmonic solver

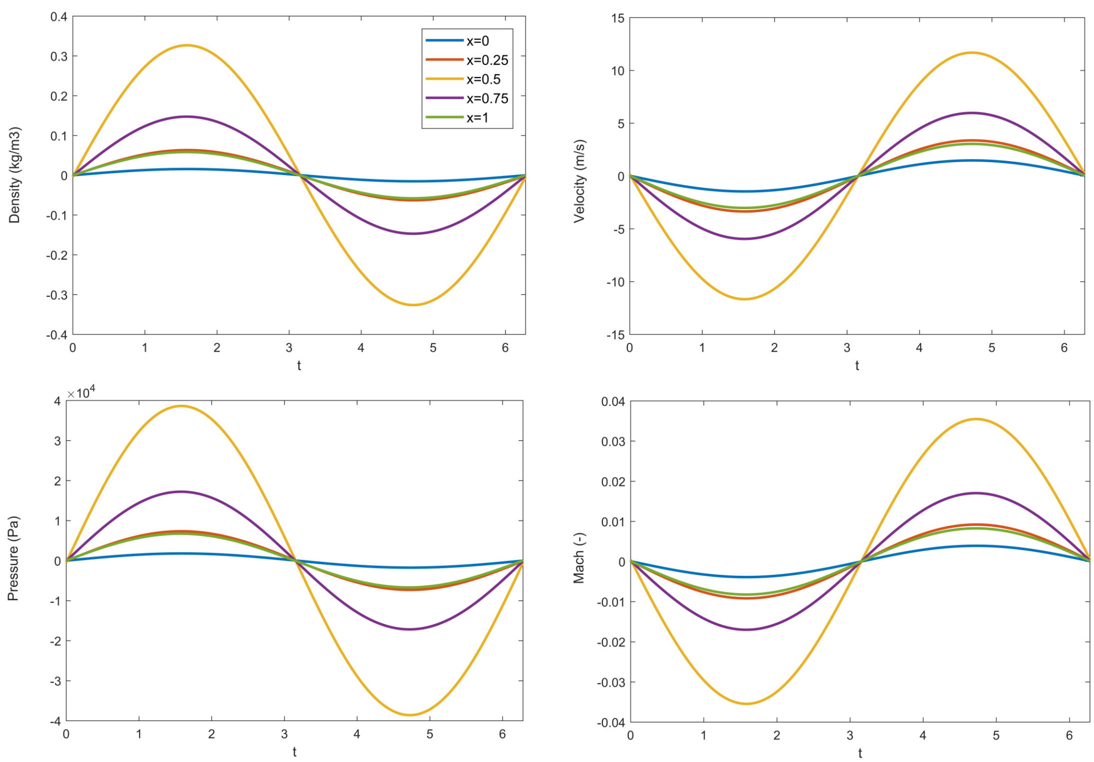

Figure 8: Perturbed primitive variables from harmonic solver

It can be seen that maximum variation from steady values occur at throat for all times and parameters. Collation of solutions for $t = 0$ and $t = T$ is obvious because of the time periodicity of the solution and physically they are the same . The important aspect observed in Figure 7 is the 180^o difference of phase angle between $\widetilde{W}_2$ and the two others. While the solution for $\widetilde{W}_1$ and $\widetilde{W}_3$ solutions reach maximum at $\frac{\pi}{4}$, $\widetilde{W}_2$ hits the bottom at that instant of time. Source of variation is the sinusoidally varying back pressure which reaches to peak at $\frac{\pi}{4}$, so $\widetilde{W}_1$ and $\widetilde{W}_3$ are in the same phase with the source while $\widetilde{W}_2$ behaves in the opposite direction. It means that, continuity and energy are related to pressure directly while momentum is related inversely which is admissible. By definition, $\widetilde{W}_1 = \tilde{\rho}$ and hence it changes in the same way as pressure changes according to ideal gas relation. Also $\widetilde{W}_2 \sim \tilde{\rho}$ and $\tilde{u}$; While $\tilde{\rho}$ is in the same phase with pressure, but $\widetilde{W}_2$ and $\tilde{u}$ are in the opposite phase, thus the role of velocity in momentum is dominant compared to density. Similarly, the same observation is made for Mach number$\tilde{M}$ which is related to $\tilde{c}$ and $\tilde{u}$. Since $\tilde{c}$ is proportional to $\tilde{\rho}$ and $\tilde{P}$, it is in the same phase with pressure while $\tilde{u}$ is not. Consequently, we can conclude that the role of variation of velocity on Mach number is dominant over variation of sound speed.

Drawing phase angle of primitive variables along nozzle, Figure 9, we can see the phase angle of pressure, density and sound speed the at end of nozzle is close to zero. Variation of pressure at the exit of nozzle is the source of variation of solution within nozzle domain. Thus, required time for affecting pressure and its directly-dependent variables will be zero at the end of nozzle. Mach number and velocity have phase angle of about π at the right end which means that they are exactly in contrast with pressure. For velocity, it is exactly the opposite to the pressure in isentropic flow. For Mach number, it occurs because it dominantly relies on velocity as mentioned above. It should be noted that phase angle must decrease as moving towards upstream direction because source of variation is at the right end and waves move in negative x direction. For instance, if harmonic pressure source is at the inlet, phase angle at the left side would be zero and increases as one moves right in positive x direction

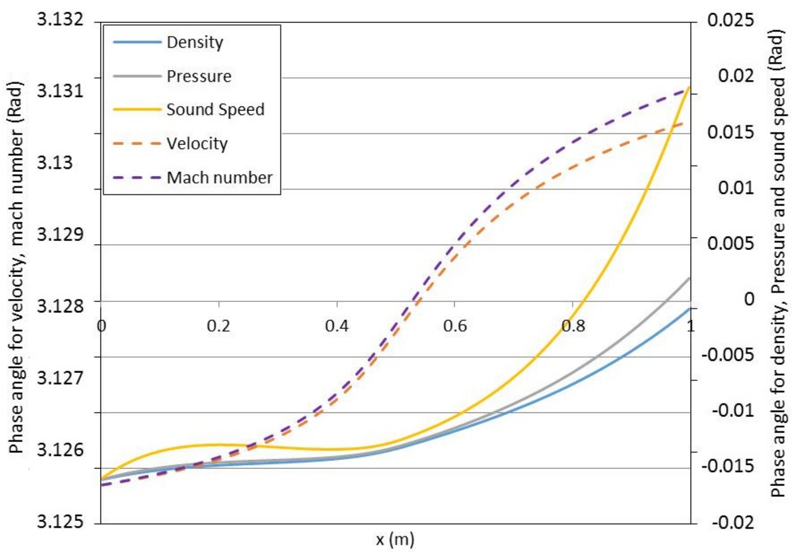

Figure 9: Phase angle of primitive variables from harmonic solver

Combining steady state results with perturbed harmonic results at specific time instants, unsteady result is obtained. Figure 10, Figure 11 and Figure 12 show unsteady density, velocity and pressure along nozzle at different instances between $t = 0$ and $t = T$.

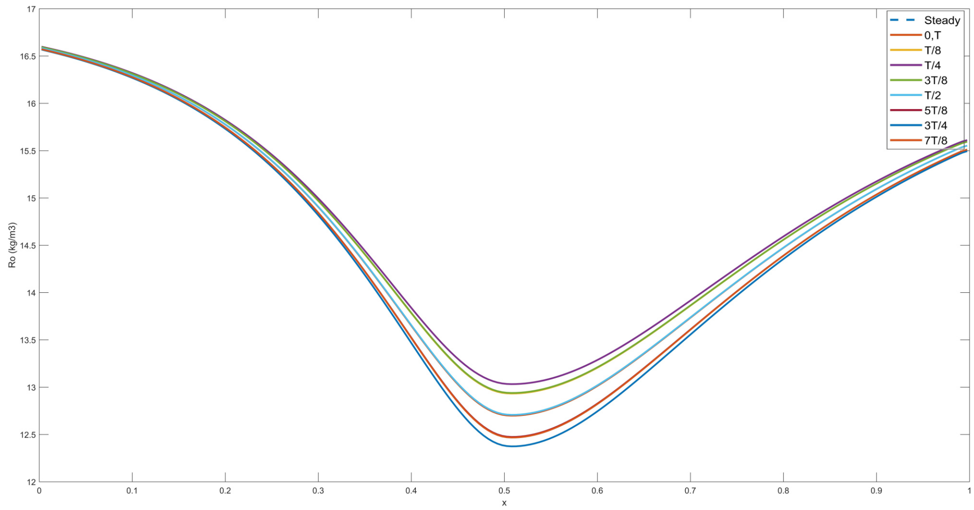

Figure 10: Unsteady density calculated by harmonic method

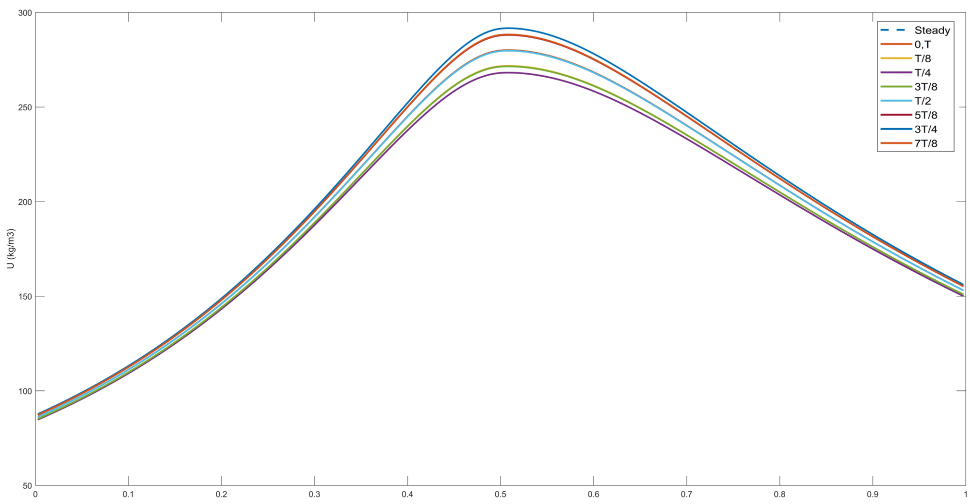

Figure 11: Unsteady velocity calculated by harmonic method

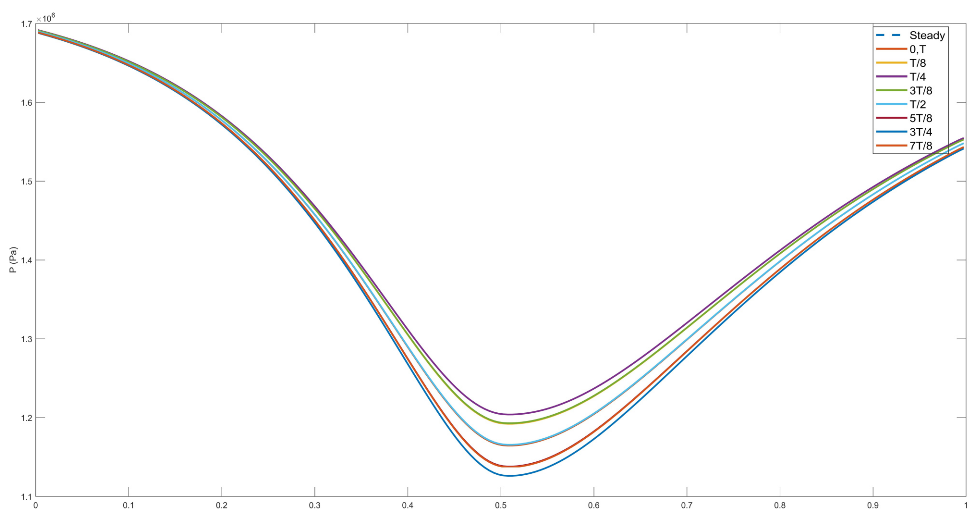

Figure 12: Unsteady pressure calculated by harmonic method

For validation, pressure distribution along nozzle is compared to unsteady time-marching results from ANSYS Fluent in which time is discretized into 100 steps for a period, thus $\Delta t = \frac{T}{100} = 0.06283185$. The comparison of pressure distribution between harmonic and time-marching methods are given in Figure 13. Similarly, in Figure 14 pressure variation with time at nozzle throat is compared for these two methods. However, time-marching is applied with three different time-steps to investigate the impact of step size on solution, 100 time-steps, 50 time steps with $\Delta t = \frac{T}{50} = 0.12566370$ and 1000 time-steps with $\Delta t = \frac{T}{1000} = 0.00628318$.

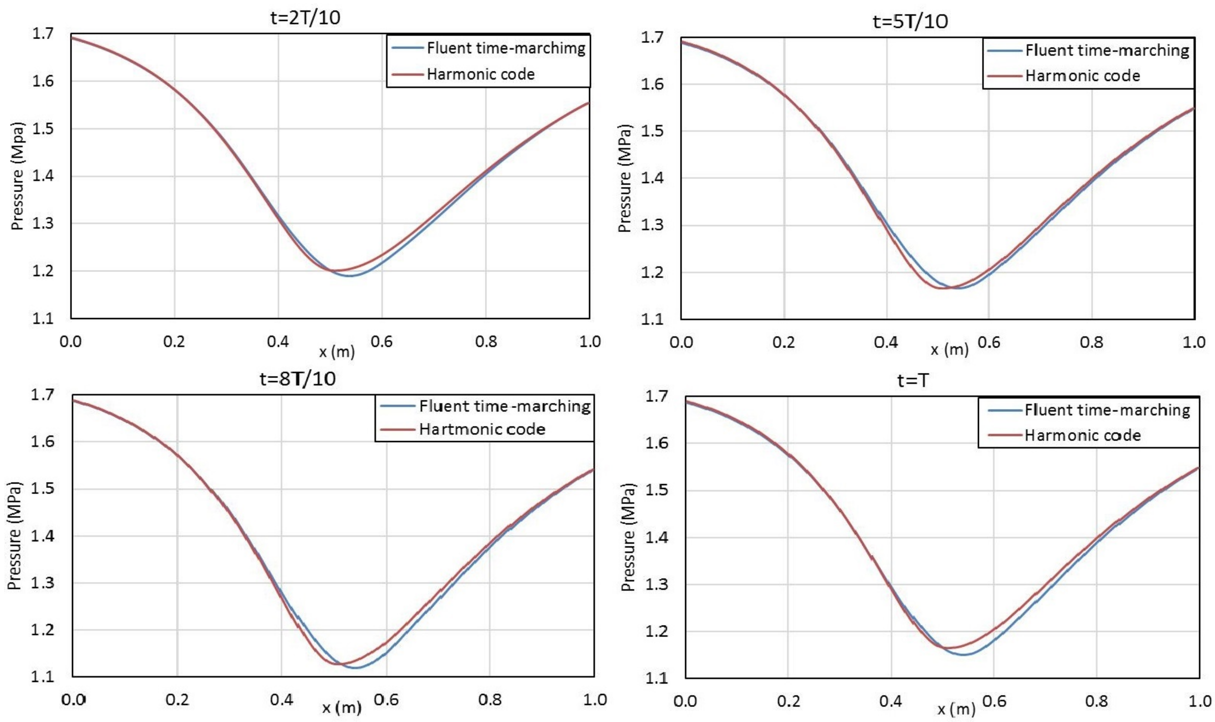

Figure 13: Comparison of solutions at different times between harmonic solver ans ANSYS Fluent

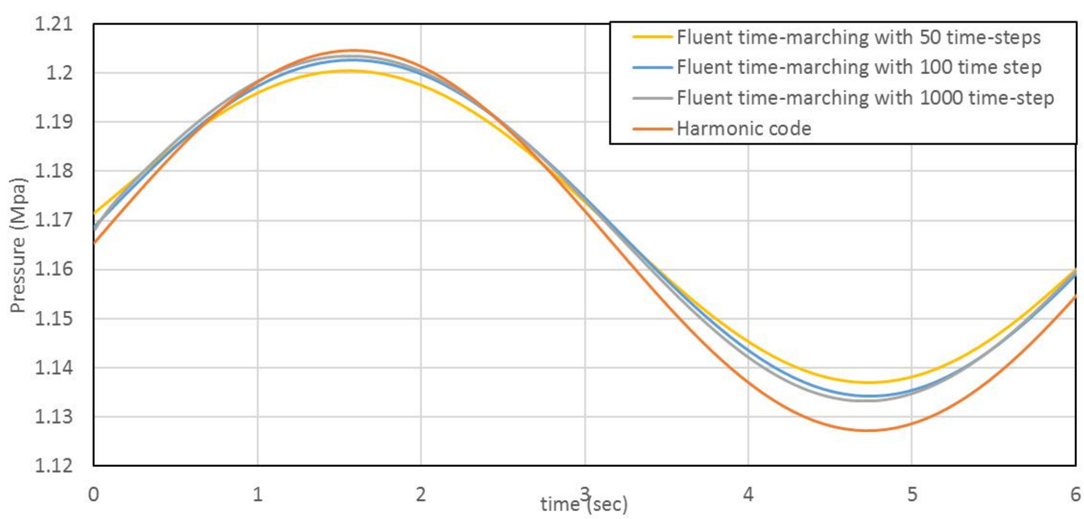

Figure 14: comparison of the unsteady results at throat by harmonic solver with ANSYS Fluent

It is seen from the figures that, harmonic solver results are in good agreement with time-marching results of Fluent. However, there are two important observations to be considered. From Figure 13, it is obvious that the magnitude of pressure from Fluent declina to the minimum value not exactly at throat, but at a location at right of the throat and is one of the reasons for having different amplitudes in Figure 14. Also, Figure 14 reveals that the size and number of time-steps in a time-marching method, influence the results. Making time-steps smaller improves the unsteady solution of time-marching method and results get closer to that obtained by harmonic method.

CONCLUSION

In this work, an unsteady subsonic compressible flow in a quasi-1D converging-diverging nozzle with sinusoidally varying back pressure is studied in frequency domain by utilizing time-linearized method. Due to increment of simultaneously solving governing equations by two times, the perturbed harmonic solution cannot be converged when either averaging or upwind methods are utilized in flux calculations across cell faces. Then harmonic solver based on Steger-Warming flux splitting method is implemented to overcome this problem. Unsteady solution obtained from time-linearized method in the frequency domain is compared to those obtained from the time-marching method from ANSYS Fluent and good agreement is observed between these two solutions. In addition, to have lower computational cost, harmonic method captures more accurate results thanks to steady form. In time-marching method, decreasing the size of time-steps improves the solution while increasing the cost of computational load. The agreement between harmonic and time marching solvers increase with decreasing time step of unsteady calculations. The other benefit of using frequency domain is the capability to obtain unsteady solution at any instant of time without limitation to time-steps that occurs in time-marching. However, applicability of this methodology is merely limited to periodic problems with a-priori frequency and amplitude while such limitation does not exist in time-marching. As the final comment, time-steps size of time-marching methodology in a periodic problem must be selected very accurately, else solution there will be a time lag in solution after several steps during convergence.

References

Adamczyk, J. and M. Goldstein (1978). Unsteady flow in a supersonic cascade with subsonic leading-edge locus. *AIAA Journal 16*(12), 1248–1254.

Hall, K. C., J. P. Thomas, and W. S. Clark (2002). Computation of unsteady nonlinear flows in cascades using a harmonic balance technique. *AIAA journal 40*(5), 879–886.

McMullen, M. S. (2003). *The application of non-linear frequency domain methods to the Euler and Navier-Stokes equations*. Ph. D. thesis, Citeseer.

Mitchell, B. E. (1995). Direct computation of the sound generated by subsonic and supersonic axisymmetric jets.

Ni, R. and F. Sisto (1976). Numerical computation of nonstationary aerodynamics of flat plate cascades in compressible flow. *Journal of Engineering for power 98*(2), 165–170.

Yao, J., A. Jameson, J. J. Alonso, and F. Liu (2001). Development and validation of a massively parallel flow solver for turbomachinery flows. *Journal of Propulsion and Power 17*(3), 659–668.